

# Stability of Efficient Deterministic Compressed Sensing for Images with Chirps and Reed-Muller Sequences

Kangyu Ni\*    Prasun Mahanti†    Svetlana Roudenko‡

## Abstract

We explore the stability of the image reconstruction algorithms with the efficient deterministic compressed sensing method. It was shown in [1] that the deterministic compressed sensing with chirps and Reed-Muller sequences for sparse 1D signals perform better than compressed sensing with random matrices and  $\ell_1$  minimization; and the algorithm with chirps is resilient to noise for sparse 1D signals. For 2D images, the assumption that the sparse signal is uniformly random no longer holds, which is required for the Statistical RIP property. Recently, we have proposed (in [20, 19, 18]) algorithms for 2D images, which are suitable when the wavelet transform is used as the sparsifying domain. It was shown that the algorithms perform well for images when the wavelet coefficients are sparse. In this work, we discuss the robustness and stability of the algorithms, specifically, when the signal is not sparse and/or when the noise is present.

**Keywords:** Compressed Sensing, Reed-Muller Sequences, FM Chirps, Image Reconstruction

## 1 Introduction

According to the theory of compressed sensing [5, 7, 12], it is possible to recover a sparse signal with a small number of measurements. There are many proposed sensing matrices and reconstruction algorithms by now, which show this is indeed feasible in practices. For instance, applications have been shown for medical images [16], communications [2], analog-to-information conversion [17], geophysical data analysis [15], etc. In the

---

\*Mathematics, Arizona State University, Tempe, AZ

†Electrical Engineering, Arizona State University, Tempe, AZ

‡Mathematics, Arizona State University, Tempe, AZ

general setting, one has  $\Phi x_0 = y$ , where  $\Phi$  is an  $n \times N$  sensing matrix,  $x_0$  is a length- $n$  signal and  $y$  is a length- $N$  measurement. The standard compressed sensing requires the sensing matrix to satisfy the Restricted Isometry Property (RIP). This means that for a fixed  $k$ , there exists a small number  $\delta_k$ , such that

$$(1 - \delta_k)\|x_k\|_{\ell_2}^2 \leq \|\Phi x_k\|_{\ell_2}^2 \leq (1 + \delta_k)\|x_k\|_{\ell_2}^2, \quad (1)$$

for any  $k$ -sparse signal  $x_k$  (at most  $k$  nonzero coefficients). Solving for the original signal  $x_0$  with  $\ell_1$  minimization,

$$\min \|x\|_{\ell_1}, \quad \text{subject to } \Phi x_0 = y, \quad (2)$$

guarantees successful recovery with a very high probability. This is a well-known theory and has been verified empirically in many papers, e.g., [7, 9]. In this paper, we explore the stability of compressed sensing, i.e., the signal may not be sparse and/or there might be a presence of noise. Compressible signals are not sparse in any transform domain but when its coefficients are sorted in the descending order,  $|x|_{(1)} > |x|_{(2)} > \dots$ , it follows a rapid decay rate,

$$|x|_{(j)} \leq \text{Const} \cdot (j + D)^{-s}, \quad (3)$$

for some power  $s \geq 1$  and shift  $D \geq 0$ . Now we review the most relevant recent results.

In [6], Candès and Romberg demonstrate that empirically it is possible to recover a compressible signal from about  $3k$  to  $5k$  projections with accuracy as good as the optimal  $k$ -term wavelet approximations. Their experiments are carried out for compressible 1D signals and 2D images. For images, they proposed a recovery algorithm that minimizes the total variation in the image domain (with  $\Psi$  the inverse wavelet transform), with  $\ell_1$ -norm constraints on the wavelet coefficients:

$$\min \|\Psi x\|_{TV} \quad \text{such that } \Phi x = y, \text{ and } \|x_j\|_{\ell_1} \leq \|x_{0_j}\|_{\ell_1}. \quad (4)$$

The  $\ell_1$ -constraints restrict the locations where the large wavelet coefficients can appear, assuming the  $\ell_1$ -values  $\|x_{0_j}\|_{\ell_1}$  of each subband  $x_{0_j} = \{x_{0_{j,m}}, m = 0, \dots, 2^{j-1} - 1\}$  are known. In their experiments, random Fourier matrices were applied to the wavelet coefficients of the images. The number of measurements are 15%, 23%, 30%, and 38% of the total number of pixels, i.e.,  $256 \times 256$ . The recovery from  $3k$  to  $5k$  random projections is comparable to the best  $k$ -term wavelet approximation.

The main results in [8] by Candès, Romberg and Tao are that the standard compressed sensing are able to stably recover sparse signals in the presence of noise in the measurements, and furthermore, stably recover compressible signals in the presence of noise. For the latter, if  $k$  is chosen

such that  $\delta_{3k}$  and  $\delta_{4k}$  in (1) satisfy  $\delta_{3k} + 3\delta_{4k} < 2$ , the error bound for compressible signals with noise in the measurements is

$$\|x_0 - \hat{x}\|_{\ell_2} \leq C_{1,k} \cdot \|\mu\|_{\ell_2} + C_{2,k} \frac{\|x_0 - x_k\|_{\ell_1}}{\sqrt{k}}, \quad (5)$$

where  $x_0$  is the true signal,  $\hat{x}$  is the recovered signal,  $x_k$  is the best  $k$ -term approximation,  $\mu$  is any perturbation, and constants  $C_{1,k}$  and  $C_{2,k}$  depend on  $\delta_{4k}$ . This theorem says that  $\ell_1$  minimization stably recovers the  $k$ -largest entries. As the authors point out, this is a deterministic statement, i.e., there is *no probability of failure*. Their experiments on both 1D and 2D compressible signals with added noise to measurements confirm this theoretical result. It is observed as well in their experiments that for small values of standard deviation of Gaussian noise, the recovery error is dominated by the approximation error, the last term in (5).

Applebaum, Howard, Searle, and Calderbank [1] proposed deterministic compressed sensing measurements by using chirp transform. In their experiments (Figs. 2 and 3 in [1]), the full pass chirp decode algorithm results in smaller reconstruction error than using Gaussian random matrices with matching pursuit. They have also shown empirically (see Fig. 4 in [1]) that these two methods are comparable when there is noise in the measurements. The 1D signals in experiments are of size  $N = 41^2$  or  $67^2$ .

Calderbank, Howard and Jafarpour [4] show that a class of deterministic sensing matrices satisfies a *statistical* restricted isometry property (StRIP), a relaxed version of the RIP property. A matrix  $\Phi$  is called  $(k, \epsilon, \delta)$ -StRIP if the inequalities

$$(1 - \delta)\|x_k\|_{\ell_2}^2 \leq \|\Phi x_k\|_{\ell_2}^2 \leq (1 + \delta)\|x_k\|_{\ell_2}^2 \quad (6)$$

hold with probability exceeding  $1 - \epsilon$  for any  $k$ -sparse vectors  $x_k$ . For example, such matrices can be constructed by chirps, Reed-Muller sequences, and BCH codes, as was done in [1, 13, 4]. An advantage of using deterministic matrices for compressed sensing is that reconstruction can be very efficient, which is shown in [1, 13] and is called the Quadratic Reconstruction Algorithm in [4]. This algorithm takes advantage of the multivariable quadratic functions that appear as exponents in the sensing matrices, and therefore, only requires vector-vector multiplication instead of matrix-vector multiplication required in Basis and Matching Pursuit algorithms that applied to random sensing matrices. The error bound of the recovered signal by the Quadratic Reconstruction Algorithm is

$$\|x_0 - \hat{x}\|_{\ell_2} \leq \frac{5 + \delta}{1 - \delta} \|x_0 - x_k\|_{\ell_2} + \frac{2}{1 - \delta} \|\mu\|_{\ell_2}, \quad (7)$$

where again  $x_0$  is the true signal,  $\hat{x}$  is the recovered signal,  $x_k$  is the best  $k$ -term approximation,  $\mu$  is the measurement noise from a Gaussian distribution, and  $\delta$  is from the StRIP property in (6). This bound  $(\ell_2/\ell_2)$  is tighter

than bounds  $(\ell_2/\ell_1)$  of random ensembles [8] and  $(\ell_1/\ell_1)$  of expander-based methods [14]. Moreover, the authors in [4] also derived that the deterministic sensing matrices are resilient to noise. We review this next.

Suppose the noise comes from the measurements, say  $y = \Phi x_k + \mu$ , where  $\mu(x)$  are iid complex Gaussian random variables with zero mean and variance  $2\sigma^2$ . Suppose  $\Phi$  satisfies

$$(1 - \epsilon')^2 \|x_k\|_{\ell_2}^2 \leq \|\Phi x_k\|_{\ell_2}^2 \leq (1 + \epsilon')^2 \|x_k\|_{\ell_2}^2 \quad (8)$$

with probability exceeding  $\delta > 0$ . Then, for  $\gamma \geq 0$ ,

$$(1 - \epsilon' - \gamma)^2 \|x_k\|_{\ell_2}^2 \leq \|y\|_{\ell_2}^2 \leq (1 + \epsilon' + \gamma)^2 \|x_k\|_{\ell_2}^2, \quad (9)$$

with probability exceeding  $1 - 2(\delta + S[\frac{\gamma\|x\|}{\sigma}])$ , where

$$S(r) = \left( \int_r^\infty e^{-y^2/2} y^{N-1} \right) \left( \int_0^\infty e^{-y^2/2} y^{N-1} \right)^{-1}. \quad (10)$$

The noisy measurement is bounded by the signal in a similar way as the inequalities in the StRIP property. Now, suppose the noise is from the signal, say  $y = \Phi(x_0 + \mu)$ , where  $\mu$  is complex multivariate Gaussian distributed, with zero mean and covariance  $E(\mu\mu^\dagger) = 2\sigma^2 I_{N \times N}$ . Then the estimates above can still be applied. Note that since  $E(\Phi\mu(\Phi\mu)^\dagger) = E(\Phi\mu\mu^\dagger\Phi^\dagger) = 2\sigma^2\Phi\Phi^\dagger$  and  $\Phi\Phi^\dagger = \frac{N}{n}I_{n \times n}$  for deterministic matrices, this has advantage over random matrices. Noise coming from the signal is harder to deal with that from the measurements because the measurement variance is a factor  $\frac{N}{n}$  larger than the source noise variance  $\sigma^2$ .

In [18], we proposed reconstruction algorithms with chirp and RM sequences sensing matrices that are suitable for 2D images. Note that while the Quadratic Reconstruction Algorithm is shown to be able to accurately reconstruct 1D sparse signals with nonzero locations chosen uniformly at random from a small number of measurements, it does not work well when is directly applied for 2D images. This is because the locations of the nonzero coefficients, usually in the wavelet domain, are not distributed uniformly. The proposed algorithm takes this into account and is shown to outperform a standard compressed sensing method, which takes random noiselet measurements and uses  $\ell_1$  minimization for reconstruction [10]. In this paper, we discuss the stability and robustness of the algorithms proposed in [18]. We show in experiments that these algorithms are stable with respect to compressible signals and robust with respect to noise.

This paper is structured as follows: in Section 2 we first discuss how to choose the proper wavelet domain and to which level an image should be decomposed into; in Section 3 we discuss the stability and robustness under noise and without sparsification. Section 4 contains the discussion of the results.

## 2 Choosing a Suitable Sparsifying Domain

We address the issue of choosing a suitable sparsifying domain for images, since the compressed sensing theory is based on the fact that the signal is sparse. Wavelets are commonly used for 2D images in compressed sensing, but the choice of a specific wavelet used is not usually discussed much. In the next subsections, we discuss how to choose a suitable Daubechies DN wavelets and a number of the decompositions. The images used in this work are shown in Figure 1, where (a) is a  $512 \times 512$  MRI image of brain, (b) is a  $512 \times 512$  MRI image of vessel, and (c) is a  $1024 \times 1024$  man image.

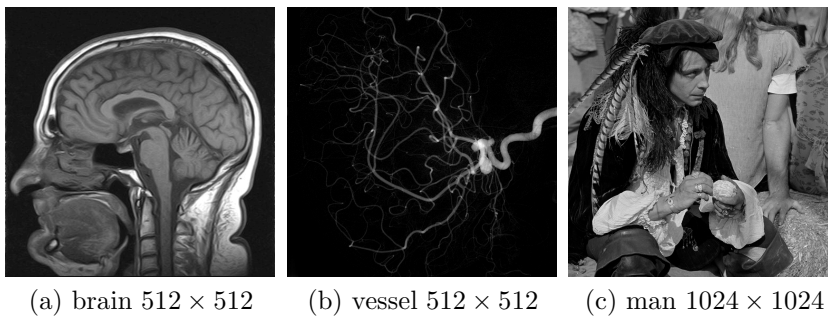


Figure 1: 2D images used in this paper

### 2.1 Daubechies DN wavelets

It is commonly believed that the Haar wavelet (D2) works best for 2D images in compressed sensing. This is because many images chosen for experiments are relatively small, i.e., at most  $128 \times 128$ . In this paper, we are interested in higher-resolution images, such as  $512 \times 512$  and  $1024 \times 1024$ . The degree of smoothness in an image loosely determines the support width of polynomials. For an image scene, if the image resolution is large, the degree of smoothness becomes large. Therefore, an appropriate support width should be large.

Figure 2 shows experiments of chirp compressed sensing using different Daubechies wavelet transforms. The vertical axis is the reconstruction SNR in dB using chirp compressed sensing. The horizontal axis shows which Daubechies wavelet DN (or  $db\frac{N}{2}$  in Matlab) is used as the sparsifying domain. The level of decompositions is fixed here and is equal to 4 levels (see explanation about the levels in Section 2.2). In particular, D2 (or db1 in Matlab) is the Haar wavelet. The 2D images are not sparsified. The number of measurements taken is 25% of the number of pixels. In all three

plots, the reconstruction SNR is optimal around D16. More strictly, the largest reconstruction SNR is within 0.5 dB from the reconstruction error at D16. The decay is faster in the vessel image (b) than in the images (a) and (c), since the vessel image is sharper than the brain and man images and contains more edges. See Table 6 in Appendix for the precise values.

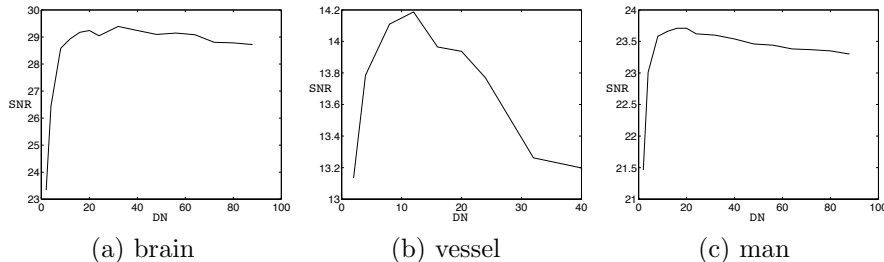


Figure 2: Reconstruction SNR (in dB) of chirp compressed sensing with different Daubechies wavelet  $DN$  (or  $\text{db}\frac{N}{2}$  in Matlab) and 4 levels of wavelet decomposition. The 2D images from Figure 1 are not sparsified. The number of measurements taken is 25% of the number of pixels.

## 2.2 Number of levels for wavelet decomposition

Figure 3 shows experiments of chirp compressed sensing using D16 with different levels of decomposition. The vertical axis is the reconstruction SNR in dB using chirp compressed sensing. The horizontal axis is the number of levels. In (a) and (c), 3 levels give the best reconstruction SNR. However, we observe that the sparsified images with 3 levels lost a lot more details than with higher levels, when compared to the original un-sparsified images. Therefore, we do not choose 3 levels. The reconstruction SNR from level 4 to 7 is within 0.1 dB range. For experiments in the next section, we thus choose 4 levels. See Table 7 in Appendix for the precise values.

## 3 Stability of the Deterministic Compressed Sensing Algorithms

By the observation in the previous section, we use Daubechies D16 with 4 levels of wavelet decomposition in all of the following experiments. To study the stability of deterministic compressed sensing using chirp and Reed-Muller sequences for 2D images under noise, we consider five cases. In the first three cases, the noise is in the sparse signal, before the transform

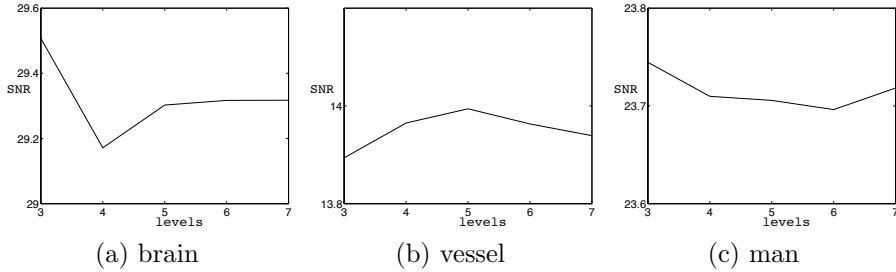


Figure 3: Reconstruction SNR (in dB) of chirp compressed sensing with Daubechies D16 wavelet and different number of levels of wavelet decomposition. The 2D images are not sparsified. The number of measurements taken is 25% of the number of pixels.

$\Phi$  is taken. In the last two cases, the noise is added after the transform. In what follows we choose noise to be i.i.d. Gaussian with mean zero and standard deviation  $\sigma$  (or in other words, the variance is  $\sigma^2$ ). The following are the cases:

1. The wavelet coefficients  $x_k$  is  $k$ -sparse. In the experiment, the 2D images are sparsified with pre-defined sparsity in the wavelet domain. The measurement is

$$y = \Phi(x_k + \mu). \quad (11)$$

2. The wavelet coefficients  $x_0$  is not sparsified, but assumed to be compressible. The measurement is

$$y = \Phi(x_0 + \mu). \quad (12)$$

3. The wavelet coefficients  $x_k$  is  $k$ -sparse and the noise  $\mu_{k^c}$  is only non-zero outside the support of  $x_k$ . Here  $k^c$  stands for the complement locations of the non-zero wavelet coefficients, i.e., the noise is added to the zero wavelet coefficients. Therefore, the nonzero coefficients of the signal are not perturbed. The measurement is

$$y = \Phi(x_k + \mu_{k^c}). \quad (13)$$

4. Noise occurs at the step of measurements and is added after the signal  $x_k$  is transformed by the CS matrix  $\Phi$ :

$$y = \Phi x_k + \mu. \quad (14)$$

5. Noise occurs at the step of measurements and is added after the compressible signal  $x_0$  is transformed by  $\Phi$ :

$$y = \Phi x_0 + \mu \quad (15)$$

Tables 1-5 show the reconstructed SNR of measurements taken according to (11)-(15), respectively. Several noise levels were chosen for the experiment; and specifically, the standard deviation  $\sigma$  of Gaussian noise with zero mean are  $\sigma = 0, 0.01, 0.05, 0.1, \text{ and } 0.2$ . These values are chosen for comparison purposes, for example, with Tables 1 and 2 in [8]. For Tables 1-3, the third columns are the SNR of the noisy images compared to the images before noise is added to the wavelet coefficients. This provides reference for the reconstructed SNR by three methods: noiselets, chirp, and RM. The first method takes random noiselet measurements and then reconstructs by  $\ell_1$  minimization. The second and third methods are deterministic compressed sensing with chirp and Reed-Muller sequences, respectively, from [18]. If noise is present in the signal, all reconstructed SNR are smaller than the reference SNR via noiselet measurements and  $\ell_1$  minimization. The reconstructed SNR by chirp has *the highest values (best)* in all cases and stay very close to the reference SNR. The reconstructed SNR by RM is higher than noiselets when the noise level is small. When the noise level is large, RM performs comparable or slightly worse than noiselets. The RM performance seems to be inconsistent with the discussion that the deterministic compressed sensing matrices comprised of chirps and Reed-Muller sequences have advantage over random matrices in Section 1. Moreover, the reconstruction algorithm is an almost  $\ell_0$  minimization, rather than the  $\ell_1$  minimization used for noiselets. The reason is that the deterministic sensing matrices here satisfy StRIP for sparse signals whose nonzero locations follow a uniform distribution, and the wavelet coefficients do not follow a uniform distribution. Therefore, better performance is not guaranteed anymore. Nevertheless, all results show the deterministic algorithms are as stable as the standard method.

For tables 4 and 5, the third columns gives the SNR of the noisy measurement compared to the clean measurement. The reconstructed SNR is calculated the same as in tables 1-3, comparing the reconstructed image to the reference image. Therefore, the SNR in the third columns is in a different domain, or differs by the  $\Phi$  transform. All results show that chirp and RM perform *significantly better* than noiselets. Note that in Tables 1, 3, and 4, where there is no noise, the reconstruction is very accurate, above 100 dB.

Table 1: The 2D images are first sparsified in the domain of Daubechies wavelet D16 (db8 in Matlab) with 4 levels of decomposition. The image, its size, and the pre-determined sparsity are shown in the first column. Gaussian noise with zero mean and variance  $\sigma^2$  (or standard deviation  $\sigma$ ) is added to the wavelet coefficients of the sparsified image; see (11). The third column shows the SNR in dB compared to the noise-free sparsified image. Columns 4 - 6 show the reconstruction SNR in dB using noiselets, chirp, and Reed-Muller CS algorithms, respectively. The number of measurements taken is 25% of the number of pixels.

image, size, sparsity	stan. dev. $\sigma$	SNR	noiselets	Chirp	RM
brain, $512 \times 512$ , 7%	0	–	29.8	127.0	121.6
	0.01	31.6	24.0	31.0	27.4
	0.05	17.7	15.4	17.1	16.1
	0.1	11.9	10.8	11.6	10.4
	0.2	6.5	6.5	6.8	5.6
vessel, $512 \times 512$ , 5%	0	–	37.1	126.2	121.0
	0.01	21.6	15.7	18.1	15.2
	0.05	8.9	7.0	7.7	6.8
	0.1	3.2	3.6	4.2	3.0
	0.2	-2.5	1.2	2.1	0.9
man, $1024 \times 1024$ , 2.38%	0	–	43.3	122.6	118.1
	0.01	32.5	30.0	32.2	30.1
	0.05	18.7	16.8	17.9	16.7
	0.1	12.9	11.8	12.5	11.3
	0.2	7.2	7.2	7.5	6.3

Table 2: In this table, the 2D images are not sparsified. Gaussian noise with zero mean and standard deviation  $\sigma$  is added to all 4 levels of D16 wavelet coefficients decomposition of the non-sparsified image; see (12). The third column shows the SNR in dB of the noisy images compared to the original image. Columns 4 - 6 show the reconstruction SNR in dB using noiselets, chirp, and Reed-Muller CS algorithms, respectively. The number of measurements taken is 25% of the number of pixels.

image, size	stan. dev. $\sigma$	SNR	noiselets	Chirp	RM
brain, $512 \times 512$	0	-	23.4	28.4	25.7
	0.01	31.6	22.2	25.7	24.6
	0.05	17.7	15.2	17.0	15.9
	0.1	12.0	10.8	11.6	10.4
	0.2	6.5	6.5	6.8	5.6
vessel, $512 \times 512$	0	-	12.0	14.1	13.4
	0.01	21.8	11.4	12.8	12.7
	0.05	9.0	6.7	7.5	6.6
	0.1	3.3	3.6	4.1	3.0
	0.2	-2.4	1.2	2.0	0.8
man, $1024 \times 1024$	0	-	20.0	23.2	22.6
	0.01	32.5	19.8	22.8	22.0
	0.05	18.8	15.2	17.3	16.1
	0.1	12.9	11.3	12.4	11.1
	0.2	7.3	7.1	7.5	6.3

Table 3: The 2D images are first sparsified in the Daubechies wavelet D16 domain with 4 levels of decomposition. The pre-determined sparsity for each image is shown in the first column. The Gaussian noise with zero mean and standard deviation  $\sigma$  is added only to the non-zero wavelet coefficients of the sparsified image; see (13). The third column shows the SNR in dB of the images with added noise compared to the noise-free sparsified image. Columns 4 - 6 show the reconstruction SNR in dB using noiselets, chirp, and Reed-Muller CS algorithms, respectively. The number of the measurements taken is 25% of the number of pixels.

image, size, sparsity	stan. dev. $\sigma$	SNR	noiselets	Chirp	RM
brain, $512 \times 512$ , 7%	0	–	29.7	127.0	121.6
	0.01	31.9	24.2	31.1	27.1
	0.05	18.0	15.5	17.1	16.1
	0.1	12.3	11.0	11.6	10.4
	0.2	6.8	6.7	6.8	5.6
vessel, $512 \times 512$ , 5%	0	–	31.7	126.2	121.0
	0.01	21.3	15.7	17.9	15.2
	0.05	8.6	7.0	7.7	6.7
	0.1	3.0	3.6	4.1	3.0
	0.2	-2.8	1.2	1.9	0.8
man, $1024 \times 1024$ , 2.38%	0	–	43.1	122.6	118.1
	0.01	35.5	29.9	32.2	30.1
	0.05	18.7	16.8	17.9	16.8
	0.1	12.8	11.8	12.6	11.3
	0.2	7.2	7.2	7.5	6.3

Table 4: The 2D images are first sparsified in the Daubechies wavelet D16 domain with 4 levels of decomposition. The pre-determined sparsity for each image is shown in the first column. Measurements are taken from the D16 domain. The number of measurement taken is 25% of the number of pixels. Gaussian noise with zero mean and standard deviation  $\sigma$  is added to the measurements of the sparsified image; see (14). The third column shows the SNR in dB of the noisy measurements compared to the noise-free measurements. Columns 4 - 6 show the reconstruction SNR in dB using noiselets, chirp, and Reed-Muller CS algorithms, respectively.

image, size, sparsity	stan. dev. $\sigma$	SNR	noiselets	Chirp	RM
brain $512 \times 512$ , 7%	0	–	29.7	127.0	121.6
	0.01	31.6	24.7	46.4	45.6
	0.05	17.6	16.8	27.5	26.8
	0.1	11.5	12.6	22.0	21.4
	0.2	5.5	8.1	15.5	14.9
vessel $512 \times 512$ , 5%	0	–	37.1	126.2	121.0
	0.01	20.6	16.4	32.8	32.7
	0.05	6.6	7.5	14.6	15.0
	0.1	0.5	2.8	10.9	10.0
	0.2	-5.5	-2.6	5.2	4.5
man $1024 \times 1024$ , 2.38%	0	–	43.1	122.6	118.1
	0.01	32.4	31.4	46.9	46.5
	0.05	18.4	18.3	27.0	26.0
	0.1	12.4	13.5	22.0	21.0
	0.2	6.4	8.6	16.0	15.5

Table 5: The 2D images are not sparsified in this experiment. Measurements are taken from the D16 domain with 4 levels of decomposition. The number of measurements taken is 25% of the number of pixels. Then, Gaussian noise with zero mean and standard deviation  $\sigma$  is added to the measurements of non-sparsified image; see (15). The third column shows the SNR in dB of the noisy measurements compared to the noise-free measurements. Columns 4 - 6 show the reconstruction SNR in dB using noiselets, chirp, and Reed-Muller CS algorithms, respectively.

image, size	stan. dev. $\sigma$	SNR	noiselets	Chirp	RM
brain $512 \times 512$	0	–	23.4	28.4	25.7
	0.01	31.6	22.4	28.0	25.7
	0.05	17.6	16.5	25.2	24.9
	0.1	11.5	12.5	21.3	20.9
	0.2	5.5	8.0	15.3	14.7
vessel $512 \times 512$	0	–	12.0	14.1	13.4
	0.01	20.6	11.5	13.8	13.4
	0.05	6.7	6.9	12.4	12.3
	0.1	0.7	2.6	9.9	9.1
	0.2	-5.3	-2.6	4.9	4.3
man $1024 \times 1024$	0	–	20.0	23.2	22.6
	0.01	32.4	19.6	23.2	22.5
	0.05	18.4	16.2	22.5	21.7
	0.1	12.4	12.7	20.2	19.4
	0.2	6.4	8.4	15.6	15.1

## 4 Discussions

In this work, we show that the algorithms introduced in [18] are stable even if the signal is not exactly sparse and there is some noise in the measurements or in the signal. We also address several practical concerns about compressed sensing with images.

First of all, the Haar wavelet is commonly used as the sparsifying transform domain. We show that it is not always the case. We compare the performance of standard Daubechies DN wavelets and suggest using Daubechies D16 as it performs the best for larger resolutions images, such as  $512 \times 512$  or  $1024 \times 1024$  pixels.

Secondly, we explain the proper selection of the number of levels for wavelet decompositions. As discussed in Section 2, levels 4-7 are optimal for wavelet decomposition, and for optimal computation time we work with level 4.

Finally, our experiments show that the algorithms are *indeed stable* if the signal is compressible and there is noise in either measurements or the signal. Furthermore, our chirp CS and RM CS reconstruction algorithms outperform the standard compressed sensing reconstruction using random matrices and  $\ell_1$  minimization. Currently, we are working on the deterministic compressed sensing algorithms to further improve their performance.

**Acknowledgments** This work is partially supported by NSF-DMS grant #0652833, NSF-DUE #0633033, and ONR-BRC grant #N00014-08-1-1110.

## Appendix: SNR values for Figures 2 and 3

Table 6: The table below shows reconstruction SNR of chirp compressed sensing with different Daubechies wavelet  $DN$  ( $=db\frac{N}{2}$  in matlab) and 4 levels of decomposition. Specifically, D2 is the Haar wavelet. The 2D images are not sparsified. Each column shows the reconstruction SNR in dB with the indicated  $DN$ . The number of measurements taken is 25% of the number of pixels. This table is plotted in Figure 2.

	D2	D4	D8	D12	D16	D20	D24	D32	D40
brain	23.34	26.45	28.58	28.93	29.17	29.24	29.04	29.39	29.24
vessel	13.13	13.79	14.11	14.19	13.97	13.94	13.77	13.26	13.12
man	21.46	23.01	23.58	23.66	23.71	23.71	23.62	23.60	23.54
	D48	D56	D64	D72	D80	D88			
brain	29.09	29.14	29.08	28.80	28.78	28.72			
man	23.46	23.44	23.38	23.37	23.35	23.30			

Table 7: The table below shows reconstruction error of chirp compressed sensing with Daubechies D16 wavelet and various levels of decomposition ranging from 3 to 7. The 2D images are not sparsified. Each column shows the reconstruction SNR in dB with the indicated number of levels. The number measurement taken is 25% of the number of pixels. This table is plotted in Figure 3.

	3	4	5	6	7
brain	29.51	29.17	29.30	29.31	29.32
vessel	13.89	13.97	13.99	13.96	13.94
man	23.74	23.71	23.71	23.70	23.72

## References

- [1] Applebaum, L., Howard, S., Searle, S., and Calderbank, R., “Chirp sensing codes: Deterministic compressed sensing measurements for fast recovery,” *Applied and Computational Harmonic Analysis* **26**, 283 – 290 (2009).
- [2] Bajwa, W. U., Haupt, J., Sayeed, A. M. and Nowak, R., “Compressed Channel Sensing: A New Approach to Estimating Sparse Multipath Channels,” in *Proc. IEEE* (June 2010)
- [3] Baraniuk, R., “Compressive sensing,” *IEEE Signal Processing Magazine* **24**, 118 – 121 (July 2007).
- [4] Calderbank, R., Howard, S. and Jafarpour S., ”Construction of a Large Class of Deterministic Sensing Matrices that Satisfy a Statistical Isometry Property”
- [5] Candès, E., “Compressive sampling,” in *International Congress of Mathematicians*, **III**, 1433–1452, European Mathematical Society, Zürich (2006).
- [6] Candès, E. and Romberg, J., ” Signal Recovery from Random Projections”, in *Proc. SPIE 5674*, 76 (2005).
- [7] Candès, E., Romberg, J., and Tao, T., “Robust uncertainty principles: Exact signal reconstruction from highly incomplete frequency information,” *IEEE Transactions on Information Theory* **52**, 489 – 509 (February 2006).
- [8] Candès, E., Romberg, J., and Tao, T., “Stable Signal Recovery from Incomplete and Inaccurate Measurements”, *Communications on Pure and Applied Mathematics*, **59**(8), pp. 1207-1223 (August 2006).
- [9] Candès, E. and Tao, T., “Near optimal signal recovery from random projections: Universal encoding strategies?,” *IEEE Transactions on Information Theory* **52**, 5406 – 5425 (December 2006).
- [10] Candès, E. and Romberg, J., “Sparsity and incoherence in compressive sampling,” *Inverse Problems* **23**(3), 969 – 985 (2007).
- [11] DeVore, R., “Deterministic constructions of compressed sensing matrices,” *Journal of Complexity* **23**, 918 – 925 (August 2007).
- [12] Donoho, D., “Compressed sensing,” *IEEE Transactions on Information Theory* **52**, 1289 – 1306 (April 2006).

- [13] Howard, S., Calderbank, A., and Searle, S., “A fast reconstruction algorithm for deterministic compressive sensing using second order Reed-Muller codes,” in [*Proceedings of the Conference on Information Sciences and Systems*], 11 – 15 (March 2008).
- [14] Indyk, P. and Ruzic, M., “Near-optimal sparse recovery in the  $\ell_1$  norm,” 49th Annual IEEE Symposium on Foundations of Computer Science, 2008 (FOCS '08), pp.199-207 (2008).
- [15] Lin, T. and Herrmann, F. J., “Compressed wavefield extrapolation”, Geophysics (August 2007).
- [16] Lustig, M., Donoho, D., and Pauly, J. M., “Sparse MRI: The application of compressed sensing for rapid MR imaging,” *Magnetic Resonance in Medicine* **58**, 1182 – 1195 (December 2007).
- [17] Mishali, M. and Eldar, Y. C., “Blind multi-band signal reconstruction: compressed sensing for analog signals”, *IEEE Trans. on Signal Processing*, 57(30), pp. 993-1009 (March 2009).
- [18] Ni, K., Datta, S., Mahanti, P., Roudenko, S. and Cochran, D., *Efficient Deterministic Compressed Sensing for Images with Chirps and Reed-Muller Sequences*, submitted to SIIMS, available at <http://math.asu.edu/kangyu/Publications.html>.
- [19] Ni, K., Datta, S., Mahanti, P., Roudenko, S. and Cochran, D., *Using Reed-Muller sequences as deterministic compressed sensing matrices for image reconstruction*, IEEE Int. Conf. on Acoustics, Speech, and Signal Processing (ICASSP), March 2010.
- [20] Ni, K., Datta, S., Mahanti, P., Roudenko, S. and Cochran, D., *Image reconstruction by deterministic compressed sensing with chirp matrices*, Proc. SPIE 7497, 74971S (2009), DOI:10.1117/12.832649
- [21] Takhar, D., Laska, J., Wakin, M., Duarte, M., Baron, D., Sarvotham, S., Kelly, K., and Baraniuk, R., “A new compressive imaging camera architecture using optical-domain compression,” in *Computational Imaging IV at SPIE Electronic Imaging*, 43 – 52 (January 2006).